Title

A sensitive bio-barcode immunoassay based on bimetallic Au@Pt nanozyme for detection of organophosphate pesticides in various agro-products

Authors

Chen, Ge
Liu, Guangyang
Jia, Huiyan
et al.

Publication Date

2021-11-01

DOI

10.1016/j.foodchem.2021.130118

Peer reviewed

HHS Public Access

Author manuscript

Food Chem. Author manuscript; available in PMC 2022 November 15.

Published in final edited form as:

Food Chem. 2021 November 15; 362: 130118. doi:10.1016/j.foodchem.2021.130118.

A sensitive bio-barcode immunoassay based on bimetallic Au@Pt nanozyme for detection of organophosphate pesticides in various agro-products

Ge Chen[a,b], **Guangyang Liu**[b], **Huiyan Jia**[c], **Xueyan Cui**[a], **Yuanshang Wang**[a], **Dongyang Li**[f], **Weijia Zheng**[a], **Yongxin She**[a], **Donghui Xu**[b], **Xiaodong Huang**[b], **A. M. Abd El-Aty**[d,e], **Jianchun Sun**[f], **Haijin Liu**[f], **Yuting Zou**[f], **Jing Wang**[a,*], **Maojun Jin**[a,g,*], **Bruce D. Hammock**[g]

[a]Institute of Quality Standard and Testing Technology for Agro-Products, Key Laboratory of Agro-Product Quality and Safety, Chinese Academy of Agricultural Sciences; Key Laboratory of Agro-Product Quality and Safety, Ministry of Agriculture Beijing 100081, P.R. China

[b]Chinese Academy of Agricultural Sciences, Ministry of Agriculture and Rural Affairs China, Key Lab Vegetables Quality and Safety Control, Institute of Vegetables & Flowers, Beijing 100081, Peoples R China

[c]Ningbo Academy of Agricultural Sciences, Ningbo, Zhengjiang 315040, P.R. China

[d]Department of Pharmacology, Faculty of Veterinary Medicine, Cairo University, 12211 Giza, Egypt

[e]Department of Medical Pharmacology, Faculty of Medicine, Atatürk University, Erzurum, Turkey

[f]Inspection and Testing Center of Agricultural and Livestock Products of Tibet, Lhasa 850000, China

[g]Department of Entomology & Nematology and the UC Davis Comprehensive Cancer Center, Davis, University of California, CA 95616, USA

Abstract

Organophosphate pesticides (OPs) are often used as insecticides and acaricides in agriculture, thus improving yields. OP residues may pose a serious threat, due to inhibition of the enzyme acetylcholinesterase (AChE). Therefore, a competitive bio-barcode immunoassay was designed for simultaneous quantification of organophosphate pesticide residues using AuNP signal amplification technology and Au@Pt catalysis. The AuNP probes were labelled with antibodies and corresponding bio-barcodes (ssDNAs), MNP probes coated with ovalbumin pesticide haptens and Au@Pt probes functionalized with the complementary ssDNAs were then prepared. Subsequently, pesticides competed with MNP probes to bind the AuNP probes. The recoveries of the developed assay were ranged from 71.26–117.47% with RSDs from 2.52–14.52%. The LODs were 9.88, 3.91, and 1.47 ng·kg^{-1}, for parathion, triazophos, and chlorpyrifos, respectively. The assay was closely correlated with the data obtained from LC-MS/MS. Therefore,

[*]**Corresponding authors: Tel.:** +86-10-8210-6570. katonking@163.com (M. J. Jin) and **Tel.:** +86-10-8210-6568; **Fax:** +86-10-8210-6567. w_jing2001@126.com (J. Wang).

the developed method has the potential to be used as an alternative approach for detection of multiple pesticides.

Keywords

Nanozyme; bio-barcode; organophosphate pesticides; Au@Pt; AuNPs

1. Introduction

Organophosphate pesticides (OPs), are widely used to defend crops against pests to boost productivity and reduce the losses. Nevertheless, the excessive application of OPs has caused critical adverse effects on human and environment (Lu et al. 2019). Their acute toxicity, as potent irreversible inhibitors of cholinesterase, may cause acute and delayed neuropathy, reproductive disorders, and endocrine disruption (Singh et al. 2020). Even though with small residual amounts, OPs could gradually accumulate in the environment along with food chain though the ecosystem cycle (Wang et al. 2021). Hence, it is essential to design a sensitive and reliable method for quantification of trace residual levels of OPs.

So far, several qualitative and quantitative analytical techniques, including gas chromatography (GC) (Fernandez-Cruz et al. 2020), gas chromatography-tandem mass spectrometry (GC−MS/MS) (Kaur et al. 2019), high-performance liquid chromatography (HPLC) (Qian et al. 2020), and liquid chromatography-tandem mass spectrometry (LC−MS/MS) (Yu et al. 2020) were designed to quantify OP residues in various agro-products. However, these techniques not only require expensive equipments and complicated operating procedures, but also need professional operators and may necessciate additional time that might limit their on-site application in agricultural products. To avoid such pitfalls, it may necessary to design a sensitive, fast, and reliable assay for determination of pesticide residues. Currently, multiple assays have been fabricated for rapid analysis of pesticide residues in various matrices. Immunoasays, such as enzyme linked immunosorbent assay (ELISA) (Esteve-Turrillas et al. 2017), chemiluminescence enzyme-linked immunoassay (CLEIA) (Chen et al. 2017; Jin et al. 2012), and fluorescence polarization immunoassay (FPIA) (Chen et al. 2017; Liu et al. 2016) have been dedicated for detection of pesticide residues. The sensitivities of the above-mentioned immunoassays are often insufficient. As previously reported, the sensitivities of immunoassay can be enhanced by bio-barcode amplification technique. The bio-barcode stategy was designed for sensitive assay of prostate-specific antigens (PSAs) without amplification by enzyme catalysis (Nam et al. 2003; Nam et al. 2004). On the basis of the aforementioned approach, Jin and co-workers have previously developed a bio-barcode immunoassay for monitoring OP residues based on polymerase chain reaction (PCR) (Du et al. 2016), digital PCR (Cui et al. 2019), fluorescent labelling technology (Zhang et al. 2018; Zhang et al. 2020; Zhang et al. 2020), and colorimetric technology (Du et al. 2017; Du et al. 2018) for agricultural products. The bio-barcode immunoassays greatly improved the sensitivity compared to common type of immunoassays. However, the above-mentioned bio-barcode immunoassay requires an appropriate amount of organic solvent. Further, antibodies or natural enzymes of these immunoassay are often more expensive, easily affected by environmental conditions when

the assay is performed, difficult to reuse, and involve a complex purification procedure (Chen et al. 2020), leading to poor reproducibility for trace determination of pesticide residues.

Nanomaterials exhibiting the catalytic activities analogous to natural enzymes are defined as nanozyme (Biswas et al.2016). Nanozyme are featured with high stability, durability, simple preparation, and low cost (Wang et al. 2020). In this context, a growing number of nanozymes have been broadly exploited in the field of food safety, owing to their tunable sizes, ease of surface modification, inherent shapes, and composite-dependent catalysis. For instance, Au nanoparticles (NPs) (Wang et al. 2011), Pd NPs (Chang et al. 2020), Pt NPs (Chen et al. 2019), Cu nanocluster (NC) (Goswami et al. 2011), Co_3O_4 NPs (Ganesamurthi et al. 2020), V_2O_5 NPs (Sasikumar et al. 2017), Fe_3O_4 NPs (Liang et al. 2013), and Au@Pt NPs (Chen et al. 2020) have been widely used in food quality control analysis, because they display high stability and efficient catalytic performance. The Pt and Au@Pt NPs were used as immunosensors with biomolecules for trace residual determination of parathion in agricultural products (Goswami et al. 2011; Chen et al. 2020). Due to the absence of specific catalytic site in nanozymes, the Pt and Au@Pt NPs are often limited to single pesticide. The nanoparticles have been utilized as immunosensors (Atar et al. 2021; Yola 2021; Medetalibeyoglu et al. 2020a; Medetalibeyoglu et al. 2020b; Yola et al. 2020) for multiple detection of pesticide residues with molecular imprinting polymer (MIP), which possess specific recognition sites for pesticides (Yola et al. 2017; Kadirsoy et al. 2020). However, the MIP requires complex preparation method. To increase the efficiency and accuracy of pesticide residue screening, an amino group functionalized 96-well black plates were used herein for detection of multiple pesticide residues. An immunosensor was prepared as follows: firstly, the AuNP probes reacted with the Au@Pt probes through complementary based pairing. Subsequently, pesticides competed with MNP probes to bind the monoclonal antibodies (mAbs) on the AuNP probes. Finally, the complex system (MNP probe and the AuNP probe) was separated by a magnetic field. The relased Au@Pt probes reacted with the carboxy modified thiol oligonucleotides in amino modofied black plate to catalyze non-fluorescent substrate of Amplex™ Red (AR) into fluorescent resorufin for OPs. The carboxy modified thiol oligonucleotides and the amino group functionalized 96-well black plate provide a strategy for multi-residue analysis of pesticides (As shown in Fig. 1). Compared to fluorescent labelled oligonucleotides, the Au@Pt nanozyme catalyzes the non-fluorescent AR substrate with a high reproducibility. In this study, a sensitive bio-barcode immunoassay based on bimetallic Au@Pt nanozyme was designed for determination of OPs in various agro-products.

2. Experimental

2.1. Materials and reagents

Pesticide standards (parathion, triazophos, and chlorpyrifos, purity >99%) were procured from Dr Ehrenstorfer (Augsburg, Germany). Chloroplatinic acid (H_2PtCl_6•$6H_2O$, >99.9%), chloroauric acid hexahydrate ($HAuCl_4$·$3H_2O$, ACS regent), and the reducing agent, sodium citrate ($C_6H_5Na_3O_7$•$2H_2O$, >99%, used during the synthetic and conjugation process) were acquired from Sigma-Aldrich (St. Louis, MO, USA). The carboxyl groups (−COOH)

functioned MNPs (10 mg·mL^{-1}) nanoparticles were secured from Invitrogen (Grand Island, NY, USA). Polyethylene glycol 20,000 (PEG 20,000), 2-(N-morpholino) acid (MES), 1-ethyl-3-[3-(dimethylamino) propyl] carbodiimide (EDC), and N-hydroxysuccinimide (NHS) were supplied by Sigma-Aldrich (St. Louis, MO, USA). L-ascorbic acid ($C_6H_8O_6$, LAA) was obtained from Fuchen (Tianjin, China). Bovine serum albumin (BSA) and OVA were provided by BBI Life Science (Shanghai, China). Tris-EDTA buffer (TE buffer, pH 8.0) was purchased from Solarbio (Beijing, China). Primary-secondary amine (PSA), octadecyl (C18), and graphitized carbon black (GCB) were picked up by Bonna-Agela Technologies (Tianjin, China). Hydrochloric acid (HCl), Nitric acid (HNO_3) and other analytical grade reagents were provided by Beijing Chemical Industry Group Co., Ltd. (Beijing, China). Analytical grade anhydrous magnesium sulphate ($MgSO_4$), sodium chloride (NaCl), and other analytical grade reagents were supplied by Sinopharm Chemical Reagent Co., Ltd. (Beijing, China). The oligonucleotides (the sequence listed in Table S1) were synthesized by Sangon Co., Ltd. (Shanghai, China). Parathion (7.57 mg·mL^{-1}), triazophos (4.53 mg·mL^{-1}), and chlorpyrifos (10.2 mg·mL^{-1}) mAbs and corresponding pesticide haptens were prepared by Zhejiang University (Hangzhou, China). A 96-well micro-plate modified with amnio group (black, flat bottom) was procured from Costar, Inc. (Kennebunk, ME, USA). The Amplex™ Red (AR) solution, acetonitrile (ACN, HPLC-grade), and methanol (MeOH, HPLC-grade) were supplied by Thermo Fisher Scientific (Pittsburgh, PA, USA). Ultrapure water was purified by Milli-QRC instrument purification system (Millipore, Bedford, MA, USA).

The buffers used in this study were prepared as following: One litre phosphate-buffered saline (PBS: 0.01 M, pH 7.4) contains KCl (0.2 g), KH_2PO_4 (0.27 g), NaCl (8 g), and Na_2HPO_4 (1.14 g). Washing buffer (PBST: 0.01 M, pH 7.4 PBS containing 0.05% Tween-20) was used for washing micro-plates, whereas, blocking buffer (0.1 M, pH 7.4, PBS containing 6% BSA) was used to block the active site. Probe buffer (0.01 M, pH 7.4, PBS, containing 2% BSA and 0.1% PEG 20,000) was used for diluting the probes. Storage buffer (0.01 M, pH 7.4, PBS with 0.02% BSA), and pesticide standard solutions diluted buffer (0.01 M, PBS and 10% methanol) were used as well throughout the experimental work.

2.2. Preparation of AuNP probes

AuNPs were synthesized according to Chen et al method (Chen et al. 2020); procedures were provided as supplemental materials. The labelled AuNP probes for the three tested OPs (parathion, triazophos, and chlorpyrifos) were prepared by simultaneously modifying the corresponding bio-barcodes and mAbs on the surface of AuNPs. The protocol used for optimization of mAb conjugated AuNPs was investigated in our previous articles (Chen et al. 2019; Chen et al. 2020). Details are stated in supplemental materials (Fig. S1) (the BSA concentration: 0.5%, the pH value: 8.5, the reaction time: 30 min, and PBS as stabilizer are the condition for bioconjugation of mAb to AuNPs). Primarily, TE buffer (27 μL, pH 8.0) and TCEP (27 μL, 20 mM) were chosen to activate bio-barcodes (ssDNA, parathion: 29.73 μg; triazophos: 29.63 μg; and chlorpyrifos: 30.26 μg) for the three tested pesticides under gentle shaking 3 h (As shown in Fig. S2). Simultaneously, 1-mL aliquot of AuNP solution was adjusted to pH 8.5 by K_2CO_3 solution (0.1 M, pH 6.0) for labelling pesticide mAbs.

Briefly, an appropriate amount of pesticide mAbs were added to the AuNP solution (to immobilize AuNPs via electrostatic interaction) and then incubated for 1 h at room temperature to form mAb-AuNP complexes. Next, the activated bio-barcodes were added into mAb-AuNP complex and incubated at 4°C for 18 h to interact with AuNPs though "Au-SH" coordination bonds to form AuNP probes. PEG 20,000 (30%, *m/v*) and PBS (0.1 M) were added to the above-mentioned AuNP probe solution to stabilize the AuNP probes. The final AuNP probe solution contains 0.5% PEG 20,000 to avoid aggregation of AuNP probes. Subsequently, 0.1 M PBS was added the above solution over 24 h to acquire final concentration of the 0.01 M PBS for stabilizing AuNP probes. Afterward, blocking buffer was added to AuNP probe solution to a BSA final concentration (0.5%, *m/v*) and then incubated at 37°C for 40 min. Excess bio-barcodes and mAbs were removed by centrifugation at 13,000 r/min, 4 °C for 30 min (Thermo Fisher Scientific, MA, USA). The precipitated AuNP probes were finally redissolved in a storage buffer for further use.

2.3. Preparation of MNP probes

An appropriate volume of pesticides OVA-haptens (50 μL for parathion, 40 μL for triazophos, and 50 μL for chlorpyrifos) was added to MNPs (10 $mg{\cdot}L^{-1}$) to prepare MNP probes as described elsewhere (Chen et al. 2020). Incipiently, NHS (500 μL, 10 $mg{\cdot}mL^{-1}$) and EDC (500 μL, 10 $mg{\cdot}mL^{-1}$) were added to a 2 mL-tube containing 50 μL MNPs. The mixture was gently shaken for 30 min, to activate the carboxyl group of MNPs. Next, the supernatant was removed under magnetic field followed by washing (3 times with 15 mM MES buffer). Subsequently, parathion OVA-hapten (50 μL), triazophos OVA-hapten (40 μL), and chlorpyrifos OVA-hapten (60 μL) conjugates were added to the activated MNPs, respectively, to form complex (shaking 18 h). The three MNP probes were washed 3 times, followed by blocking the MNP probes using blocking buffer for 60 min. Then, the blocked MNP probes were suspended in 1 mL of 0.01 M PBS (pH 7.4, containing 0.1% Tween-20 and 0.1% BSA) to prepare MNP probes that were stored at 4°C for further analysis.

2.4. Preparation of Au@Pt probes

The Au@Pt nanoparticles were synthesized as described elsewhere (Chen et al. 2020). Firstly, 30 mL AuNP solution (prepared in section 2.2) was chosen as a seed. Then, H_2PtCl_6 (1.0 mM, 10 mL) and L-ascorbic acid (5 mM, 10 mL) were added, respectively, and boiled under mild stirring. Au@Pt was entirely prepared when the solution changed from wine-red to brown-red. The prepared Au@Pt was filtered through a cellulose nitrate filter before preparation of the Au@Pt nanozyme probes. As for the preparation of AuNP probes, the complementary bio-barcodes (C-ssDNA, parathion: 30.50 μg; triazophos: 30.33 μg; and chlorpyrifos: 30.22 μg) require activation prior reaction with Au@Pt (1 mL) solution to produce the Au@Pt probes. Similarly, a mixture of 30% PEG 20000 and 3% BSA was added to the above Au@Pt solution to achieve a final concentration (0.5% PEG 20000 and 1% BSA) for stabilizing the Au@Pt probes within 24 h. Afterward, excess C-ssDNA was discarded by centrifugation at 13, 000 r/min for 30 min (4°C). Au@Pt probes were stored at 4°C pending further analysis.

2.5. Competitive bio-barcode immunoassay

A competitive bio-barcode immunoassay was catalysed by Au@Pt nanozyme. Firstly, 100 μL AuNP probes diluted with probe buffer at an optimal concentration was added to tubes. Subsequently, Au@Pt probes (100 μL) were added and incubated in humidity chamber (1 h, 37°C). Afterward, 40 μL pesticide standards diluted to a series of concentrations (by diluted buffer or samples extract supernatant) were added to Au@Pt probe solution, followed by the addition of 40 μL modified MNP probes to establish the competitive immunoassay (at 37°C, 30 min). The above complex was washed 3 times using washing buffer, separated under magnetic field, and then blocked by 60 μL blocking buffer under 75% humidity (at 37°C, 1 h). Thereafter, the complex was shaken (at 60 °C, 1 h) to untie the bio-barcodes at a high temperature and low salt conditions. Finally, the released Au@Pt probes interacted with the carboxy modified thiol oligonucleotides in amino modified black plate to catalyse non-fluorescent AR substrate into fluorescent resorufin for analysis of OPs.

2.6. Sample pre-treatments

The cabbage, apple, pear, and rice samples were procured from the Beijing supermarkets to assess the performance of the bio-barcode immunoassay based on bimetallic Au@Pt nanozyme for multiple residual detection. Blank samples (confirmed by LC-MS/MS to be free from the target analytes, parathion, triazophos, and chlorpyrifos) were used for preparation of calibration curve and spike-and-recovery experiments. The quick, easy, cheap, effective, rugged, safe (QuEChERS) method designed by Anastassiades and coworkers was used as a sample pre-treatment procedure (Anastassiades et al. 2003) with minor modifications. Three different mixed standard concentrations (10, 50, and 100 $\mu g \cdot kg^{-1}$) were spiked to homogenized samples (10 g, accurate to 0.01g) in 50-mL tubes. Subsequently, the mixture was mixed well and equilibrated at room temperature (in the absence of light) for 4 h. Next, 10 mL acetonitrile was added followed by 2 min shaking. Afterwards, 4 g anhydrous $MgSO_4$ and 1 g NaCl were added to above mixture (supernatant for dehydration and stratification) after vigorous shaking for 1 min. Then, the supernatant was transferred into a 10-mL plastic tube after centrifuging at 10,000 r/min (6 min). Subsequently, 3 mL supernatant was purified using dispersive solid-phase adsorbents (150 mg of PSA, 150 mg of C18, and 7.5 mg of GCB) after high-speed shaking for 30 s, and then centrifuged at 10,000 r/min (at 4 °C, 5 min). Finally, the supernatant was dried under stream of nitrogen and then reconstituted in 10% methanol-PBS for bio-barcode immunoassays. For LC-MS/MS analysis, the supernatant was filtered through a 0.22-μm membrane (Jinteng, China) into a glass auto-sampler vial.

3. Results and discussion

3.1. Optimization of the bio-barcode sequences

The chain length of bio-barcodes is the key factor for nanozyme catalysis activity. As shown in Table S2 and Fig. S3, the catalytic activity of nanozyme reached to maximum fluorescence when the chain length of bio-barcode was 35 bp. The chain length of bio-barcodes was too short, leading to the reactions among oligonucleotides are difficult. Whereas, the catalytic active site of the nanozyme is obscured with the long chain length of bio-barcodes.

3.2. Characterization of AuNP probes

The morphology of AuNP probes were characterized by transmission electron microscopy (TEM) and energy-dispersive spectrometry (EDS). As shown in Fig. 2 (A), the AuNPs were spherical in shape with uniform size, forming dark core surrounded by shadow coating. These data revealed that mAbs and ssDNA were successfully conjugated on AuNPs surfaces. Meanwhile, the AuNP probes were also accessed by EDS to qualitatively evaluate the characteristic elements. The results of EDS analysis have shown C, N, P, and S chemical signals as presented in Fig. 2 (B). The characteristic elements, P and S, can be inferred from ssDNA and pesticide mAbs, respectively. The AuNPs has a maximum absorption peak (520 nm) as shown in Fig. S4. Further, the UV-vis spectroscopy of AuNPs probes is shown in Fig. S5 with 260 nm and 280 nm peak (red line). These results denote that AuNPs were successfully modified with ssDNA and mAbs.

3.3. Characterization of Au@Pt probes

It is crucial to synthesize Au@Pt probes with superior and sometimes unprecedented properties to improve the sensitivity of bio-barcode immunoassay. The synthesis of Au@Pt (AuNPs were used as seeds) was prepared through deposition of a thin Pt layer on the surface of AuNPs. Similar to AuNPs and AuNP probes, the Au@Pt probes were characterized by TEM, EDS, and UV-vis spectroscopy. As shown in Fig. 3 (A), The TEM of Au@Pt exhibited good dispersion with average diameters of 20 nm. The flocculant Au@Pt particle size was increased by approximately 5 nm compared to smooth AuNPs, indicating the existence of smooth AuNPs surface of a 5 nm layer Pt to form Au@Pt (As shown in Fig. S6).

In a similar way, the EDS analyses of Au@Pt probes have P chemical element except for Au, Pt, C, N, and O element (As shown in Fig. 3(B)). The analysis showed that P element was derived from the complementary bio-barcodes (C-ssDNA), denoting that the complementary bio-barcodes (C-ssDNA) were successfully modified on Au@Pt surfaces. As AuNPs, the Au@Pt has a maximum absorption peak (510 nm) as shown in Fig. S4. Further, the UV-vis spectroscopy of Au@Pt probes is shown in Fig. S5 with 260 nm peak (black line). The above results denote that the nanozyme Au@Pt probes were successfully fabricated for further experimental works.

3.4. Optimal concentrations of mAbs

The sensitivities of the immunoassay based on nanozyme Au@Pt rely on the concentrations of mAbs modified on AuNPs, as more mAbs on the AuNPs can greatly improve the affinity to react with antigens. Thereby, the concentrations of OPs mAbs conjugated on AuNPs were optimized in the immunoassay based on Au@Pt nanozyme. A series of concentration of mAbs was designed for preparation of different AuNP probes, with final respective concentrations of 7.57, 22.71, 45.42, 68.13, 113.55, and 136.26 mg for parathion; 4.53, 9.06, 22.65, 45.30, 67.95, and 91.54 mg for triazophos; and 30.6, 61.2, 91.8, 122.4, 153, and 183.6 mg for chlorpyrifos. The fluorescence intensity was measured after competitive immunoassay reaction. The results demonstrated that as the mAbs concentrations increased, the fluorescence intensity increases first, and then decreases. Further, the ability to specifically recognize the pesticide hapten or pesticide was decreased, when the amount

of mAb on AuNPs was low. Notably, there is steric hindrance for higher concentrations of mAbs modified on AuNPs that would affect the interplay between bio-barcode and AuNPs. Thence, the optimal concentrations of mAbs were found to be 45.42, 22.65, and 91.80 mg for parathion, triazophos, and chlorpyrifos, respectively (Fig. 4).

3.5. Optimization of probe working concentrations

The probe (AuNP and MNP) concentrations play a key role in the sensitivity of bio-barcode immunoassay based on Au@Pt nanozyme. Thus, optimizing the probe concentrations is necessitated to create calibration curves. The concentrations of AuNP probes were 4.54, 2.27, and 1.14 $mg{\cdot}L^{-1}$ for parathion. Similarly, the concentrations were 2.27, 1.13, and 0.57 $mg{\cdot}L^{-1}$ for triazophos, and 9.18, 4.59, and 2.30 $mg{\cdot}L^{-1}$ for chlorpyrifos. Additionally, a series of MNP probes diluted at 5.0, 1.25, and 0.63 $mg{\cdot}L^{-1}$ was separately established for competitive bio-barcode immunoassay based on Au@Pt nanozyme (As shown in Table S3). The value represents the maximum fluorescence intensity (Fmax) to IC_{50} (the concentration of analyte, inhibiting 50% of fluorescent tracer binding) ratio was used to assess the optimal working concentrations of bio-barcode immunoassay. The higher sensitivity with lower IC_{50} and higher $Fmax/IC_{50}$ value. For parathion, the optimal working concentrations were 2.27 $mg{\cdot}L^{-1}$ for AuNP and 0.63 $mg{\cdot}L^{-1}$ for MNP probes. Additionally, the optimal working concentrations of AuNP and MNP probes were 1.13 and 0.63 $mg{\cdot}L^{-1}$ for triazophos and 4.59 and 1.25 $mg{\cdot}L^{-1}$ for chlorpyrifos, respectively.

3.6. Calibration curves

Calibration curves were designed for the developed bio-barcode immunoassays based on Au@Pt. Under the optimized conditions, the fluorescence intensity was measured (in triplicate) as a function of pesticide concentrations. The results revealed that the fluorescence intensity decreased and the inhibition of pesticide increased as the concentrations of pesticides increased. Pesticides and the MNP probes were added to the AuNP probes at the same time because hapten labelled on MNP probes and pesticides may compete for the limited antibody on the AuNP probes. Excess pesticides are removed by washing procedure. Calibration curves and their regression equations were established using Origin 9.0 (Inhibition (%) as Y as an ordinate axis and the logarithmic (LOG) concentration of pesticides as the X abscissa axis). The results are shown in Fig. 5 and Table S4. The calibration curves exhibited good linearity with RSDs <14.34% (parathion, $y = 21.373x + 52.859$, R^2=0.9796; triazophos, $y = 18.023x + 53.391$, R^2= 0.9615; and chlorpyrifos, $y = 21.516x + 49.426$, R^2 = 0.9713). The IC_{50} values were 0.74, 0.65, and 1.06 $\mu g{\cdot}kg^{-1}$, whereas the IC_{10} values (IC_{10} is the concentration of pesticide causing 10% inhibition in the maximum fluorescence) were 9.88, 3.91, and 1.47 $ng{\cdot}kg^{-1}$ for parathion, triazophos, and chlorpyrifos, respectively. Moreover, comparison of the assay sensitivity for parathion, triazophos, and chlorpyrifos with nanozyme as probe is listed in Table S5. These results indicate that the designed immunoassay has high sensitivity for multiple OPs residue detection.

3.7. Accuracy and precision

The accuracy (expressed as recovery), precision (expressed as relative standard deviation: RSD), and the limits of detection (LOD) were used to evaluate the reliability and

applicability of the immunoassay. Three concentrations (10, 50, and 100 μg·kg^{-1}) of pesticide standard solutions (parathion, triazophos, and chlorpyrifos) were spiked to blank samples (cabbage, apple, pear, and rice) to estimate recovery rate, which reflects the accuracy of the bio-barcode immunoassay based on Au@Pt nanozyme and LC-MS/MS (LC-MS/MS conditions are provided in Table S6). The precision was assessed under optimized conditions. The average recoveries of the developed bio-barcode immunoassay based on Au@Pt nanozyme were ranged from 71.26% to 117.47% with RSDs in between 2.35%−14.52%. This finding denotes that the designed bio-barcode immunoassay meets the requirements for determination of pesticide residues. These results were in a good agreement with those determined by LC–MS/MS (Recovery rate: 70.04–106.72% and RSD: 0.6–9.87%) (Table S7). The above results were acceptable for pesticide residue analysis in agro-products. Moreover, the regression equations were obtained from standard curves established using blank matrix supernatant. Regression equations were used to evaluate the correlation of bio-barcode immunoassay based on Au@Pt nanozyme catalysis. For bio-barcode immunoassay based on Au@Pt nanozyme catalysis, the R^2 ranged from 0.9494–0.9862, the IC_{50} from 1.09 to 2.86 μg·kg^{-1}, and the LOD from 3.95×10^{-3} to 25.84×10^{-3} ng·kg^{-1} (Table S8). The cross-reactivity between the tested pesticides (parathion, triazophos, and chlorpyrifos) with the unrelated (other than parathion, triazophos, and chlorpyrifos) pesticides has been reported in our previous work (Chen et al. 2019; Chen et al. 2020; Zhang et al. 2018). There is no cross-reactivity among these pesticides with the unrelated pesticides. These results demonstrate that the bio-barcode immunoassay based on Au@Pt nanozyme catalysis is a reliable method for detecting OPs residues.

3.8. Confirmation analysis

To assess the correlation coefficients of the bio-barcode immunoassay based on Au@Pt nanozyme with a LC-MS/MS method, rice and cabbage samples were randomly selected for confirmation test. Blank samples (n=30) from rice and cabbages were spiked with pesticide mixtures (parathion, triazophos, and chlorpyrifos) at 10, 50, and 100 μg·kg^{-1}. The samples were mixed thoroughly, and half of the samples were tested by the designed bio-barcode immunoassay and the rest was analysed using LC-MS/MS. Thereafter, the correlation coefficients of the two analytical methods were assessed. The correlation coefficients in rice were 0.9843, 0.9630, and 0.9536 for parathion, triazophos, and chlorpyrifos, respectively. For cabbage, the correlation coefficients were 0.9643, 0.9676, and 0.9783, respectively (Fig. 6). These results reveal that the bio-barcode immunoassay based on Au@Pt nanozyme catalysis has a good reliability and accuracy to meet the requirements for pesticide detection.

4. Conclusions

A selective fluorescence immunoassay based on Au@Pt nanozyme was designed for multi-residue detection of OPs. The Au@Pt nanozyme can directly catalyzes the AR substrate without a classical enzyme labelling procedure. Further, we found that the carboxy modified thiol oligonucleotides and amino modified black plate provided high sensitivity and selectivity. Overall, this immunoassay exhibits the potential as a sensitive and reliable method for trace residual detection of pesticides and small molecules in various agricultural products.

Supplementary Material

Refer to Web version on PubMed Central for supplementary material.

Acknowledgments

This study was financially supported by National Key Research Program of China (No. 2019YFC1604503), NIEHS Superfund Research Program (No. P42 ES04699), and Ningbo Innovation Project for Agro-Products Quality and Safety (No. 2019CXGC007)

References

Anastassiades M, Lehotay SJ, tajnbaher D, Schenck FJ (2003). Fast and easy multiresidue method employing acetonitrile extraction partitioning and dispersive solid-phase extraction for the determination of pesticide residues in produce. Journal of AOAC International. 86, 412–430. [PubMed: 12723926]

Atar N, Yola ML (2021). A novel QCM immunosensor development based on gold nanoparticles functionalized sulfur-doped graphene quantum dot and h-ZnS-CdS NC for Interleukin-6 detection. Analytica Chimica Acta. 1148:3338202.

Biswas S, Tripathi P, Kumar N, Nara S (2016). Gold nanorods as peroxidase mimetics and its application for colorimetric biosensing of malathion. Sensors and Actuators, B: Chemical. 231, 584–592.

Chang FC, Huang JW, Chen CH (2020). Au-Pt-Pd spherically self-assembled nano-sieves as SERS sensors. Journal of Alloys and Compounds. 843, 9.

Chen G, Jin MJ, Du PF, Zhang C, Cui XY, Zhang YD, She YX, Shao H, Jin F, Wang SS, Zheng LF, Wang J (2017). A sensitive chemiluminescence enzyme immunoassay based on molecularly imprinted polymers solid-phase extraction of parathion. Analytical Biochemistry. 530, 87–93. [PubMed: 28499497]

Chen G, Jin M, Ma J, Yan M, Cui X, Wang Y, Zhang X, Li H, Zheng W, Zhang Y, Abd El-Aty AM, Hacimuftuoglu A, Wang J (2020). Competitive bio-barcode immunoassay for highly sensitive detection of parathion based on bimetallic nanozyme catalysis. Journal of Agricultural and Food Chemistry. 68 (2), 660–668. [PubMed: 31804828]

Chen G, Jin M, Yan M, Cui X, Wang Y, Zheng W, Qin G, Zhang Y, Li M, Liao Y, Zhang X, Yan F, Abd El-Aty AM, Hacimuftuoglu A, Wang J (2019). Colorimetric bio-barcode immunoassay for parathion based on amplification by using platinum nanoparticles acting as a nanozyme. Microchimica Acta.186 (6), 339. [PubMed: 31073796]

Chen QM, Zhang XD, Li SQ, Tan JK, Xu CJ, Huang YM (2020). MOF-derived Co_3O_4@Co-Fe oxide double-shelled nanocages as multi-functional specific peroxidase-like nanozyme catalysts for chemo/biosensing and dye degradation. Chemical Engineering Journal. 395, 10.

Chen YS, Cui XP, Wu PP, Jiang ZY, Jiao LY, Hu QQ, Eremin SA, Zhao SQ (2017). Development of a homologous fluorescence polarization immunoassay for diisobutyl phthalate in romaine lettuce. Food Analytical Methods. 10 (2), 449–458.

Cui X, Jin M, Zhang C, Du P, Chen G, Qin G, Jiang Z, Zhang Y, Li M, Liao Y, Wang Y, Cao Z, Yang F, Abd El-Aty AM, Wang J (2019). Enhancing the sensitivity of the bio-barcode immunoassay for triazophos detection based on nanoparticles and droplet digital polymerase chain reaction. Journal of Agricultural and Food Chemistry. 67 (46), 12936–12944. [PubMed: 31670953]

Du P, Jin M, Chen G, Zhang C, Cui X, Zhang Y, Zhang Y, Zou P, Jiang Z, Cao X, She Y, Jin F, Wang J (2017). Competitive colorimetric triazophos immunoassay employing magnetic microspheres and multi-labeled gold nanoparticles along with enzymatic signal enhancement. Microchimica Acta. 184 (10), 3705–3712.

Du P, Jin M, Zhang C, Chen G, Cui X, Zhang Y, Zhang Y, Zou P, Jiang Z, Cao X, She Y, Jin F, Wang J (2018). Highly sensitive detection of triazophos pesticide using a novel bio-barcode amplification competitive immunoassay in a micro well plate-based platform. Sensors and Actuators, B: Chemical. 256, 457–464.

Du P, Jin M, Chen G, Zhang C, Jiang Z, Zhang Y, Zou P, She Y, Jin F, Shao H, Wang S, Zheng L, Wang J (2016). A competitive bio-barcode amplification immunoassay for small molecules based on nanoparticles. Scientific Reports. 6.

Esteve-Turrillas FA, Mercader JV, Agullo C,Abad-Somovilla A, Abad-Fuentes A (2017). A class-selective immunoassay for simultaneous analysis of anilinopyrimidine fungicides using a rationally designed hapten. Analyst. 142 (20), 3975–3985. [PubMed: 28956038]

Fernandez-Cruz T, Alvarez-Silvares E, Dominguez-Vigo P, Simal-Gandara J; Martinez-Carballo E (2020).Prenatal exposure to organic pollutants in northwestern Spain using non-invasive matrices (placenta and meconium). Science of the Total Enviroment. 731, 12.

Ganesamurthi J, Keerthi M, Chen SM, Shanmugam R (2020). Electrochemical detection of thiamethoxam in food samples based on Co_3O_4 nanoparticle@graphitic carbon nitride composite. Ecotoxicology and Enviromental Safety. 189, 9.

Goswami N, Giri A, Bootharaju MS, Xavier PL, Pradeep T, Pal SK (2011). Copper quantum clusters in protein matrix: potential sensor of Pb^{2+} ion. Analytical Chemistry. 83 (24), 9676–9680. [PubMed: 22050123]

Jin MJ, Shao H, Jin F, Gui WJ, Shi XM, Wang J, Zhu GN (2012). Enhanced competitive chemiluminescent enzyme immunoassay for the trace detection of insecticide triazophos. Jounal of Food Science. 77 (5), T99–T104.

Kadirsoy S, Atar N, Yola ML (2020). Molecularly imprinted QCM sensor based on delaminated MXene for chlorpyrifos detection and QCM sensor validation. New Journal of Chemistry. 44:6524–6532.

Kaur R, Kaur R, Rani S, Malik AK, Kabir A, Furton KG (2019). Application of fabric phase sorptive extraction with gas chromatography and mass spectrometry for the determination of organophosphorus pesticides in selected vegetable samples. Journal of Separation Science. 42 (4), 862–870. [PubMed: 30600583]

Liang M, Fan K, Pan Y, Jiang H, Wang F, Yang D, Lu D, Feng J, Zhao J, Yang L, Yan X (2013). Fe_3O_4 magnetic nanoparticle peroxidase mimetic-based colorimetric assay for the rapid detection of organophosphorus pesticide and nerve agent. Analytical Chemistry. 85 (1), 308–312. [PubMed: 23153113]

Lu X, Tao L, Li Y, Huang H, Gao F (2019). A highly sensitive electrochemical platform based on the bimetallic Pd@Au nanowires network for organophosphorus pesticides detection. Sensors and Actuators B: Chemical. 284, 103–109.

Liu Y, Liu R, Boroduleva A, Eremin S, Guo YR, Zhu GN (2016). A highly specific and sensitive fluorescence polarization immunoassay for the rapid detection of triazophos residue in agricultural products. Analytical Methods. 8 (36), 6636–6644.

Medetalibeyoglu H, Beytur M, Akyıldırım O, Atar N, Yola ML (2020). Validated electrochemical immunosensor for ultra-sensitive procalcitonin detection: carbon electrode modified with gold nanoparticles functionalized sulfur doped MXene as sensor platform and carboxylated graphitic carbon nitride as signal amplification. Sensors and Actuators B: Chemical. 319:128195.

Medetalibeyoglu H, Kotan G, Atar N, Yola ML (2020). A novel and ultrasensitive sandwich-type electrochemical immunosensor based on delaminated MXene@AuNPs as signal amplification for prostate specific antigen (PSA) detection and immunosensor validation. Talanta. 220:121403.

Nam JM, Thaxton CS, Mirkin CA (2003). Nanoparticle-based bio-bar codes for the ultrasensitive detection of proteins. Science. 301 (5641), 1884–1886. [PubMed: 14512622]

Nam JM, Stoeva SI, Mirkin CA (2004). Bio-bar-code-based DNA detection with PCR-like sensitivity. Journal of the American Chemistry Society. 126 (19), 5932–5933.

Qian H, Yang Q, Qu Y, Ju ZW, Zhou WF, Gao HX (2020). Hydrophobic deep eutectic solvents based membrane emulsification-assisted liquid-phase microextraction method for determination of pyrethroids in tea beverages. Journal of Chromatography A. 1623, 9.

Sasikumar R, Govindasamy M, Chen SM, Chieh-Liu Y, Ranganathan P, Rwei SP (2017). Electrochemical determination of morin in Kiwi and Strawberry fruit samples using vanadium pentoxide nano-flakes. Journal of Colloid and Interface Science. 504, 626–632. [PubMed: 28618382]

Singh J, Thakur S, Singh R, Kaur V (2020). Schiff base-Zn2+ ion combo as 'pick and degrade' probe for selected organophosphorus chemical weapon mimics and flame retardant analog: detoxification of fruits and vegetables in aqueous media. Food Chemistry. 327, 8.

Wang J, Duan HL, Fan L, L., Zhang J, Zhang ZQ (2021). A magnetic fluorinated multiwalled carbon nanotubes-based QuEChERS method for organophosphorus pesticide residues analysis in Lycium ruthenicum Murr. Food Chemistry. 338, 127805.

Wang W, Gunasekaran S (2020). Nanozymes-based biosensors for food quality and safety. Trends in Analytical Chemistry. 126.

Wang XX, Wu Q, Shan Z, Huang QM (2011). BSA-stabilized Au clusters as peroxidase mimetics for use in xanthine detection. Biosensors & Bioelectronics. 26 (8), 3614–3619. [PubMed: 21382705]

Yola ML (2021). Sensitive sandwich-type voltammetric immunosensor for breast cancer biomarker HER2 detection based on gold nanoparticles decorated Cu-MOF and Cu2ZnSnS4NPs/Pt/g-C3N4 composite. Microchimica Acta. 188:78. [PubMed: 33569679]

Yola ML, Atar N (2020). Amperometric galectin-3 immunosensor-based gold nanoparticle-functionalized graphitic carbon nitride nanosheets and core–shell Ti-MOF@COFs composites. Nanoscale, 12:19824–19832. [PubMed: 32966539]

Yola ML, Atar N (2017). A highly efficient nanomaterial with molecular imprinting polymer: carbon nitride nanotubes decorated with graphene quantum dots for sensitive electrochemical determination of chlorpyrifos. Journal of The Electrochemical Society, 164 (6):B223–B229.

Yu CC, Hao DY, Chu Q, Wang T, Liu SN, Lan T, Wang FH, Pan CP (2020). A one adsorbent QuEChERS method coupled with LC-MS/MS for simultaneous determination of 10 organophosphorus pesticide residues in tea. Food Chemistry. 321, 8.

Zhang C, Du P, Jiang Z, Jin M, Chen G, Cao X, Cui X, Zhang Y, Li R, Abd El-Aty AM, Wang J (2018). A simple and sensitive competitive bio-barcode immunoassay for triazophos based on multi-modified gold nanoparticles and fluorescent signal amplification. Analytical Chimica Acta. 999, 123–131.

Zhang C, Jiang Z, Jin M, Du P, Chen G, Cui X, Zhang Y, Qin G, Yan F, Abd El-Aty AM, Hacimuftuoglu A, Wang J (2020). Fluorescence immunoassay for multiplex detection of organophosphate pesticides in agro-products based on signal amplification of gold nanoparticles and oligonucleotides. Food Chemistry. 326.

Zhang X, Du P, Cui X, Chen G, Wang Y, Zhang Y, Abd El-Aty AM, Hacimuftuoglu A, Wang J, He H, Jin M, Hammock B (2020). A sensitive fluorometric bio-barcodes immunoassay for detection of triazophos residue in agricultural products and water samples by iterative cycles of DNA-RNA hybridization and dissociation of fluorophores by Ribonuclease H. Science of The Total Environment. 717.

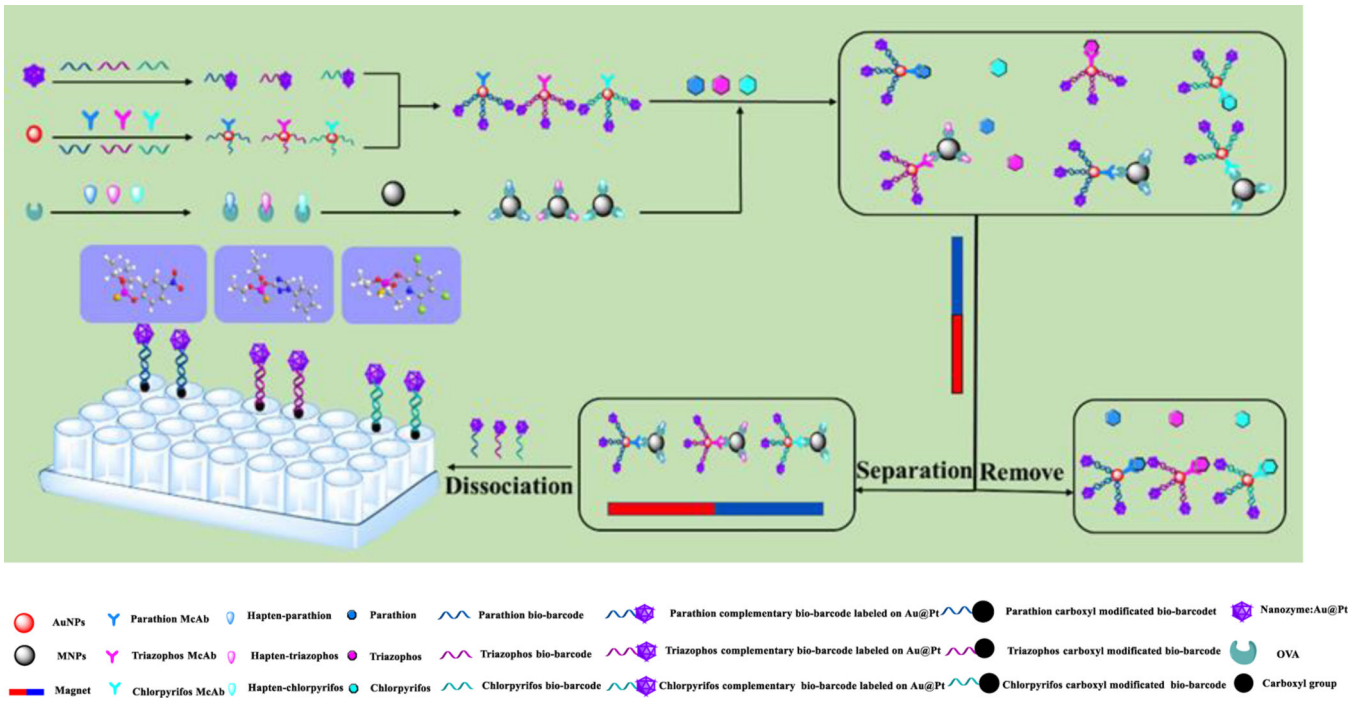

Fig. 1.

Schematic illustration of fluorescent bio-barcode immunoassays for detection of OPs based on amplification by Au@Pt nanozyme.

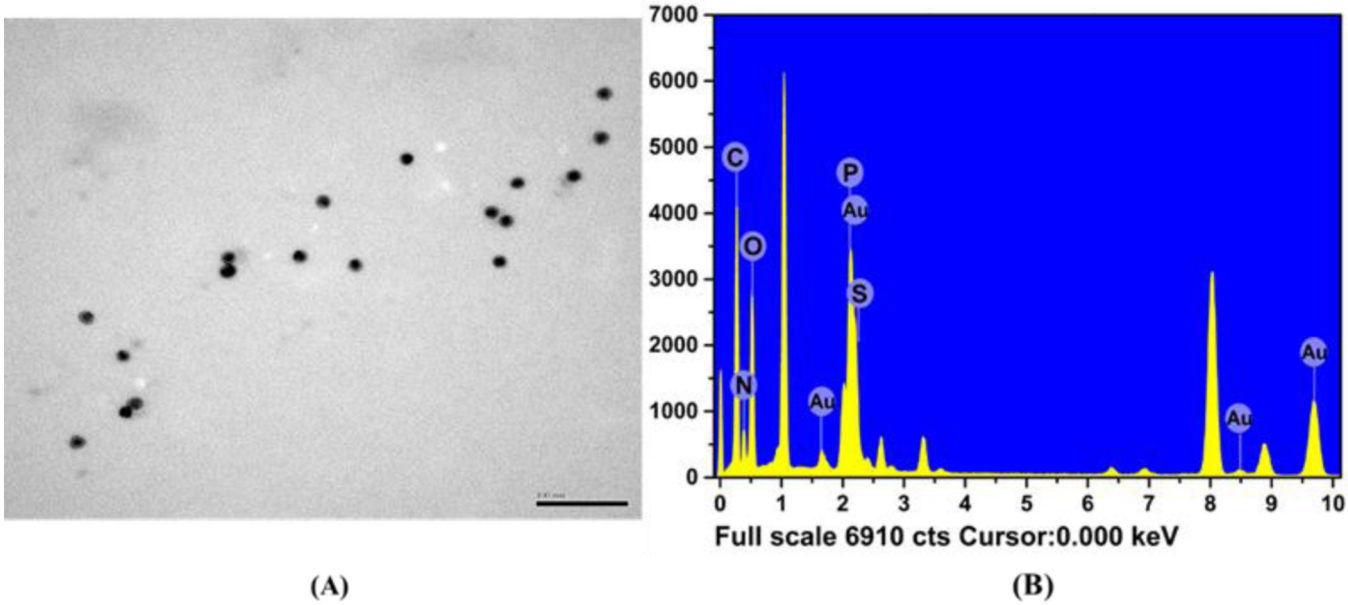

Fig. 2.
Characterization of Au probe (A): TEM and (B): EDS images.

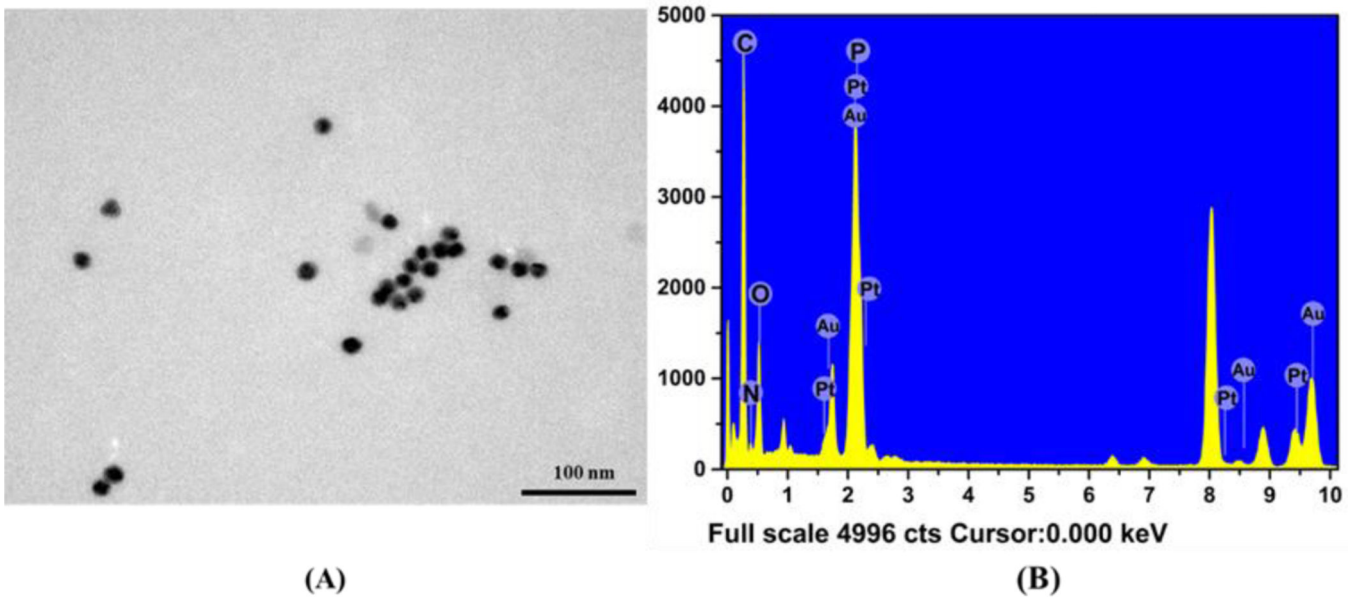

Fig. 3.
Characterization of Au@Pt probe (A) TEM and (B) EDS images

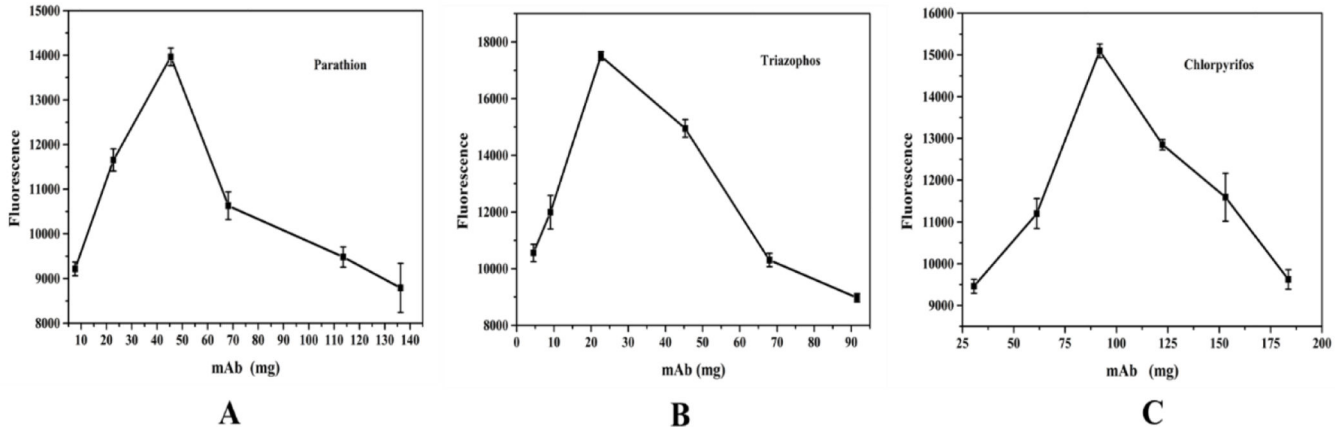

Fig. 4.

The optimization of concentration of antibodies pesticides (A) parathion, (B) triazophos and, (C) chlorpyrifos labelled on AuNPs (n=3)

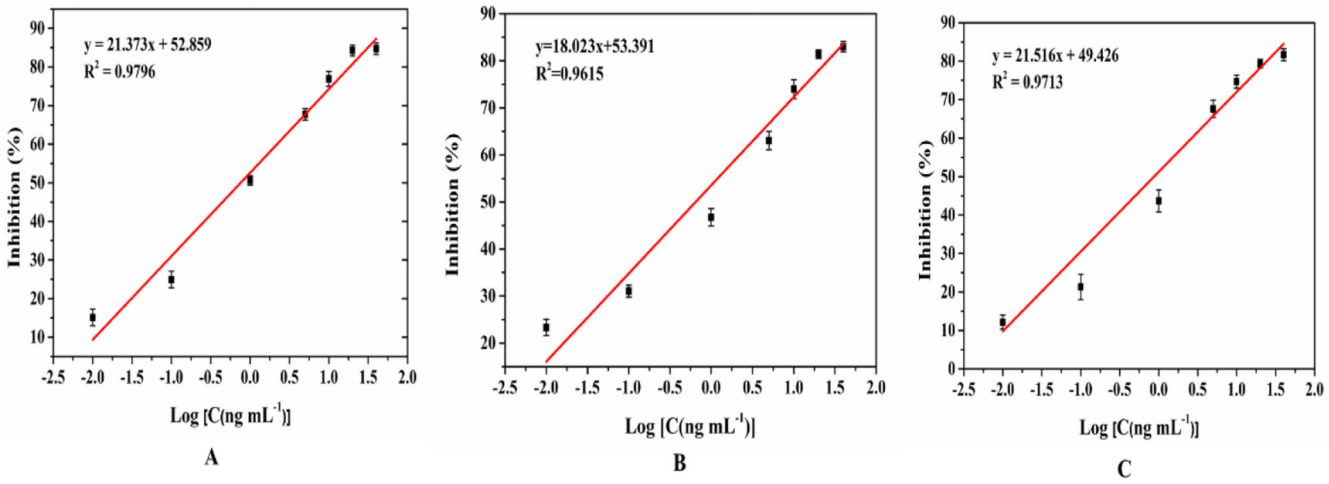

Fig. 5.

The calibration curves of bio-barcode immunoassay for (A) parathion, (B) triazophos, (C) chlorpyrifos (n=3).

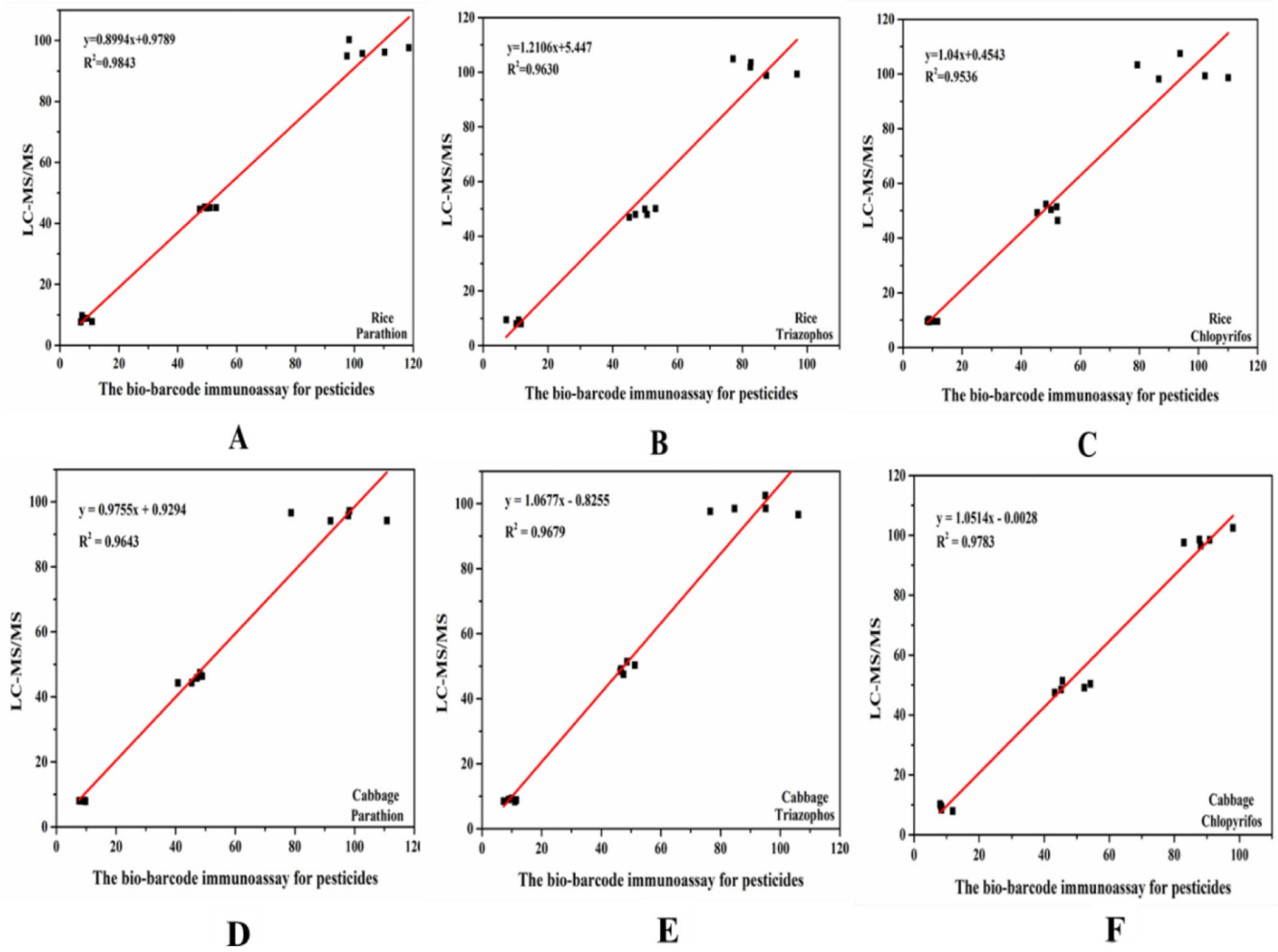

Fig. 6.

Correlation coefficients between the concentrations of parathion, triazophos, and chlorpyrifos measured by bio-barcode immunoassay and LC-MS/MS in rice and cabbage samples.